

**Zr-2.5Nb**                       **$K_{IH}$**

**$K_{IH}$  Dependence on Hydrogen Concentration and Orientation in  
CANDU Zr-2.5Nb Tubes**

150

Zr-2.5Nb                      delayed hydride cracking (DHC)  
 (threshold stress intensity factor),  $K_{IH}$   
 ,                      160-280 °C                      .                      compact  
 tension                      ,                      ,                       $K_{IH}$                       20  
 MPa√m                      60-100 ppm                      .                       $K_{IH}$                       20  
 0.5 MPa√m                      Zr-2.5Nb                       $K_{IH}$                       가 30 ppm  
 .                      8.4 MPa√m                      5.8 MPa√m  
 .                      가 30 ppm  
 가                       $K_{IH}$                       .  
                     Zr-2.5Nb                       $K_{IH}$

Abstract

The threshold stress intensity factor,  $K_{IH}$  of the CANDU Zr-2.5Nb tubes were investigated in their radial and axial directions as a function of the hydrogen concentration at temperatures ranging from 160 to 280 °C. Compact tension and cantilever beam specimens that were electrolytically charged to 60 to 100 ppm hydrogen were used to determine the axial and radial  $K_{IH}$ , respectively. The  $K_{IH}$  were determined using a load-decreasing method where the applied stress intensity factor decreased from 20 MPa√m step-wisely by 0.5 MPa√m until no crack

growth was detected by an acoustic emission sensor or the direct current potential drop method. The  $K_{IH}$  of CANDU Zr-2.5Nb tubes in the radial direction was  $8.4 \text{ MPa}\sqrt{\text{m}}$  which is higher than that in the axial direction or  $5.8 \text{ MPa}\sqrt{\text{m}}$  at the supersaturated hydrogen concentration in excess of around 30 ppm H. However, when the supersaturated hydrogen concentration was less than 30 ppm H, the  $K_{IH}$  exponentially increased with the decreasing supersaturation of hydrogen concentration. The  $K_{IH}$  dependence on the orientation and the hydrogen concentration was discussed from viewpoints of the angle between the hydride habit plane and the cracking plane and a hydride fracture stress dependence on the hydride size.

1.

Zr-2.5Nb 가 rolled joint  
DHC (delayed hydride cracking)  
Zr-2.5Nb RBMK Zr-2.5Nb  
[1], 가 가  
DHC 가  
가  
[2]. Zr-2.5Nb DHC 가 가  
DHC (threshold stress  
intensity factor),  $K_{IH}$  , Zr-2.5Nb  $K_{IH}$   
가  
 $K_{IH}$

2.

4 800 °C 11:1 20-  
25% 가 (cold drawing) 400 24 Zr-2.5Nb  
 $K_{IH}$  20.4 mm 17mm compact  
tension 3.5 mm 38 mm  
[3,4].  
KAERI [5]. 가  
가가  $K_{IH}$

60, 80 100 ppm H 가 , 1  
 (acoustic emission) , compact tension  
 (direct current potential drop method)  $K_{IH}$   
 12-25 MPa√m 20 MPa√m  
 가 2  
 : 0.5-5 °C/min  
 310-380 °C 1  
 1-2 °C/min  
 30 20 MPa√m 20  
 MPa√m 0.5 MPa√m  
 가 ,  
 $K_{IH}$   
 $K_{IH}$  DHC  
 KAERI [5]

3.

### 3.1. $K_{IH}$

3 280 °C Zr-2.5Nb  $K_{IH}$   
 가 60 ppm ,  $K_{IH}$  가 ,  
 가 100 ppm  $K_{IH}$  가 .  
 $K_{IH}$  Shi가 Kim DHC  
 [6], DHC  
 3  $K_{IH}$   
 280 °C (terminal solid solubility for dissolution of hydrogen)  
 ,  $\Delta C$  (= -  
 or 280 °C TSSD)  $K_{IH}$  ( 4).  
 4  $K_{IH}$  ,  $\Delta C$ 가 30 ppm 5  
 ,  $\Delta C$ 가 30 ppm  
 280 °C 160-250 °C  $K_{IH}$  ,  
 $\Delta C$  Zr-2.5Nb  $K_{IH}$   
 ,  $\Delta C$   
 $K_{IH}$ 가 4 5  
 30 ppm H 160-280 °C Zr-

2.5Nb (TSSD) , Pan [7] TSSP (TSSP)-  
가 26.3 ppm 5 8.4-26.3ppm  
30 ppm 가  
가 가  
 $K_{IH}$  가 4  
 $K_{IH}$  가 ,  $\Delta C$ 가  
가 TSSP-TSSD  
가 ,  $\Delta C$   
3-5  $K_{IH}$  가  
3.2.  $K_{IH}$  4 5  $K_{IH}$  8.4±0.7  
MPa√m 5.8±0.4MPa√m (95% )  $K_{IH}$ 가  
 $K_{IH}$ 가  
[8],  
[9]. ,  $K_{IH}$ 가  $K_{IH}$  가  
6  
6 가

$K_{IH}$ 가  $K_{IH}$

4. Zr-2.5Nb DHC  $K_{IH}$

$\Delta C$   $\Delta C$ 가 30 ppm

. 30 ppm ,  $\Delta C$

– (=TSSP-TSSD) ,  $\Delta C$   $K_{IH}$

$\Delta C$ 가  $K_{IH}$

가

$K_{IH}$

$K_{IH}$  8.4±0.7 MPa√m

5.8±0.4MPa√m  $K_{IH}$

$K_{IH}$  가

1. Y.S. Kim et al., "Delayed Hydride Cracking Velocity of TMT-1 Zr-2.5Nb Pressure Tube", KAERI/TR-1941/2001 (2001).
2. KINS, "1" (1994).
3. S. Sagat, C.E. Coleman, M. Griffiths and B.J.S. Wilkins, "Zirconium in the Nuclear Industry, Tenth International Symposium, ASTM STP 1245, p.89, (1994).
4. S.J. Kim, Y.S. Kim, K.S. Im, S.S. Kim and Y.M, Cheong, "Delayed Hydride Cracking of Zr-2.5Nb tubes with the Notch Tip Shape and Cooling Rate", J.Kor. Inst. Met.& Mater., 41, 21 (2003).
5. Y.S. Kim et al., "A Manual for Characterization Tests for Zr-2.5Nb Pressure Tubes", KAERI Technical Report, KAERI/TR-1329/99 (1999).
6. Y.S. Kim et al., "DHC Velocity and  $K_{IH}$  of Zr-2.5Nb Tubes with Hydrogen", Journal of Metals, 55 (2), 383 (2003).
7. Z.L. Pan, I.G. Ritchie and M.P. Puls, "The Terminal Solid Solubility of Hydrogen and Deuterium in Zr-2.5Nb Alloys", J. Nucl. Mater., 228, 227 (1996).
8. Y.S. Kim, S.C. Kwon and S.S. Kim, "Crack Growth Pattern and Threshold Stress Intensity

- Factor, KIH, of Zr-2.5Nb Alloy with the Notch Direction”, Nucl. Mater., 280, 304 (2001).
9. Y.S. Kim, Y. Perlovich, M. Isaenkova, S.S. Kim and Y.M. Cheong, “Precipitation of Reoriented Hydrides and Textural Change of  $\alpha$ -Zirconium Grains during Delayed Hydride Cracking of Zr-2.5%Nb Pressure Tube”, J. Nucl. Mater., 297, 292 (2001).

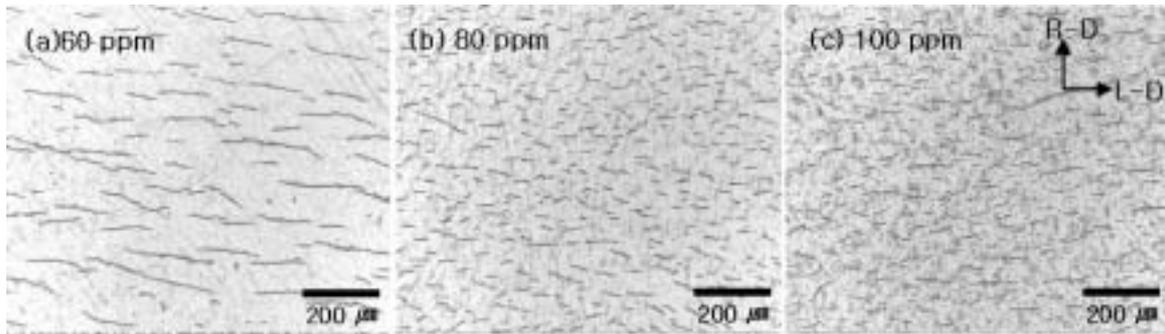


Fig. 1. Distribution of hydrides precipitated in the specimens after charging of 60, 80 and 100 ppm H.

$T_{\text{test}}$  varied from 260 to 280 °C

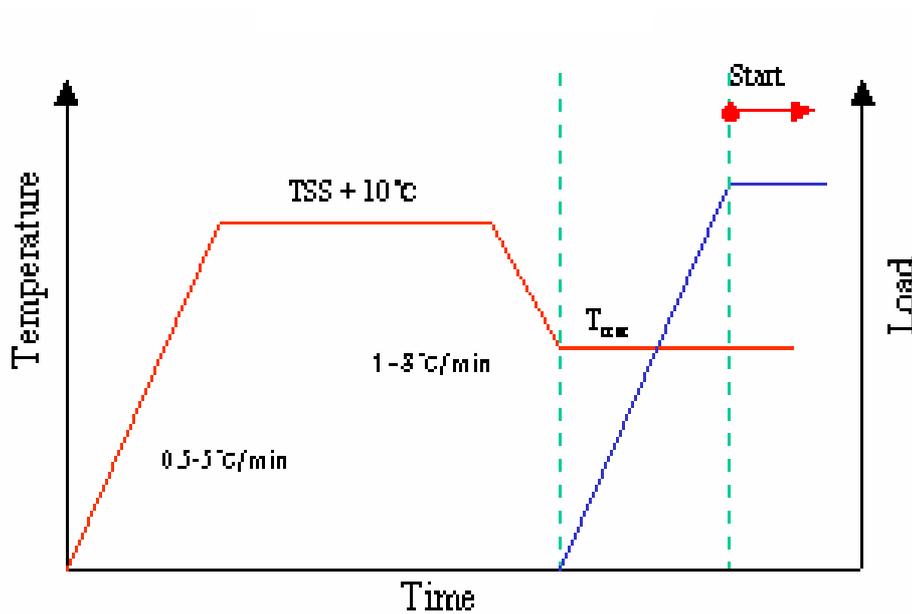


Fig. 2. Schematic diagram of a thermal cycle and loading schedule applied during DHC tests.

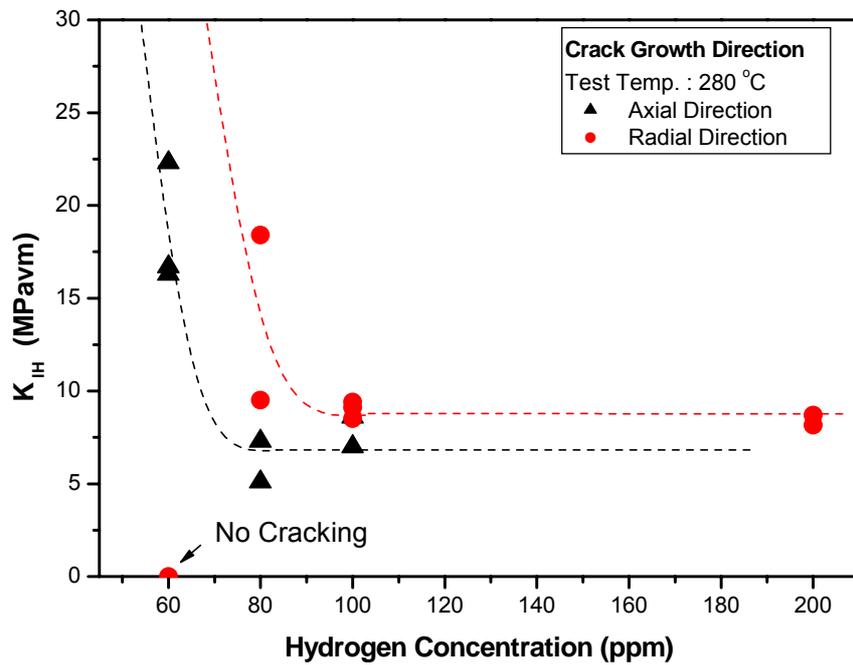


Fig. 3. Axial and radial threshold stress intensity factors,  $K_{IH}$  at 280 °C of the Zr-2.5Nb tube with the total charged hydrogen concentration.

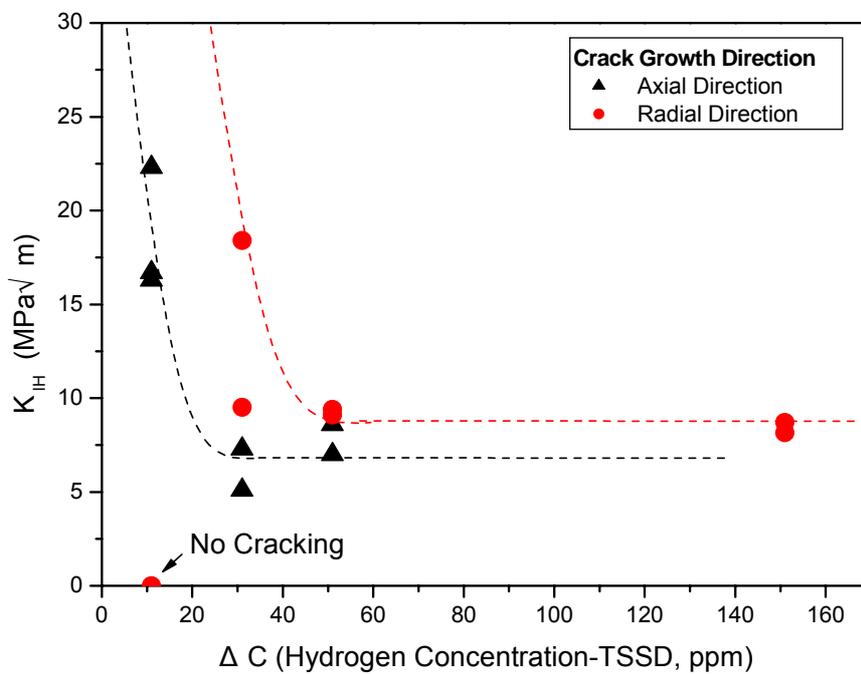


Fig. 4. Threshold stress intensity factors,  $K_{IH}$  at 280 °C of the Zr-2.5Nb tube with the supersaturated hydrogen concentration or  $\Delta C$  over the terminal solid solubility for dissolution of hydrogen at 280 °C.

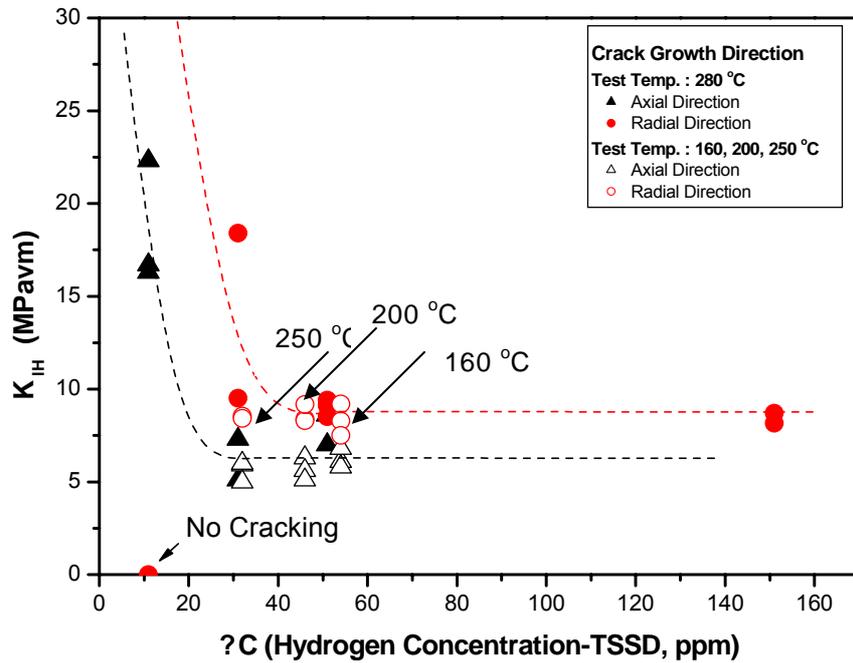


Fig. 5.  $K_{IH}$  of the CANDU Zr-2.5Nb tube as a function of the supersaturated hydrogen concentration,  $\Delta C$  over the terminal solid solubility for dissolution at various temperatures.

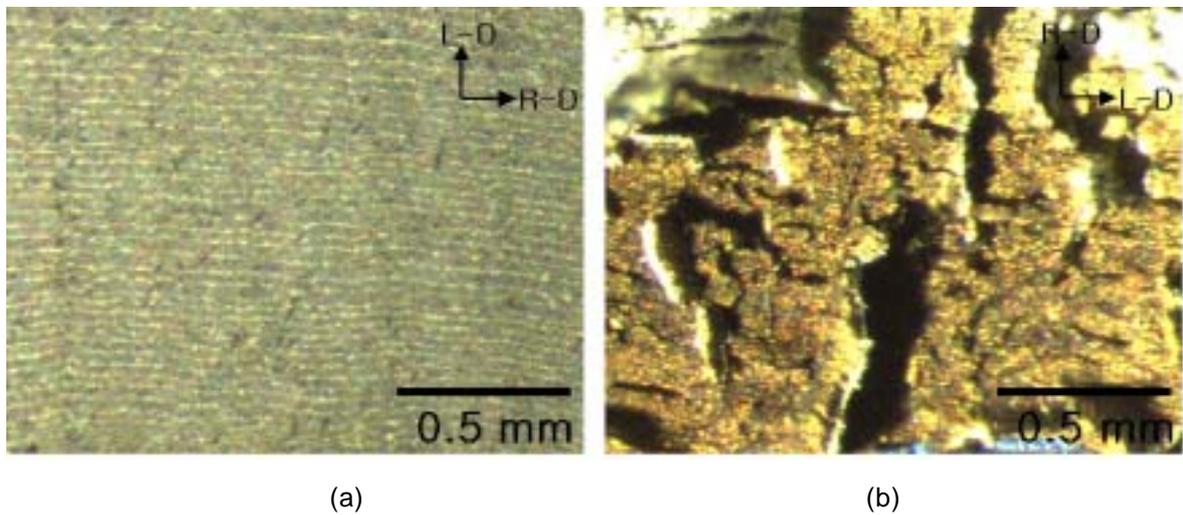


Fig. 6. DHC fracture pattern of the CANDU Zr-2.5Nb tube with the orientation: Flat fracture surface was observed on the CT specimens where the DHC crack grew in the axial direction while the rugged fracture surface appeared on the cantilever beam specimen where the DHC crack grew in the radial direction.